Strontium Aluminate Persistent Luminescent Single Crystals: Linear Scaling of Emission Intensity with Size Is Affected by Reabsorption

David van der Heggen, Jonas J Joos, Daniel Rytz, Bruno Viana, Philippe F Smet

Strontium Aluminate Persistent Luminescent Single Crystals: Linear Scaling of Emission Intensity with Size is Affected by Reabsorption.

David Van der Heggen,[1] Jonas J. Joos,[1] Daniel Rytz,[2] Bruno Viana,[3] Philippe F. Smet[1]

[1] LumiLab, Department of Solid State Sciences, Ghent University, Krijgslaan 281/S1, 9000 Gent, Belgium
[2] BREVALOR Sàrl, Impasse des Frênes 1, CH-1669 Les Sciernes, Switzerland
[3] PSL Research University, Chimie ParisTech, IRCP, CNRS, 75005 Paris, France

Abstract: The green-emitting $SrAl_2O_4$:Eu,Dy phosphor is the most widely-used and well-studied persistent luminescent phosphor available today. Recent efforts to boost its performance in terms of luminescence intensity and duration are challenged by complex loss mechanisms, including the optically stimulated release of previously trapped charges by excitation light. Here we present minimally scattering $SrAl_2O_4$:Eu,Dy single crystals which, as opposed to powder phosphors, allow to profit from a so-called volume effect, resulting in significantly increased emission intensity. Additionally, they allow to identify the reabsorption of the afterglow emission by trapped charges as an important loss mechanism, leading to a non-linear scaling of the emission intensity with the crystal size. If circumvented, the emission intensity could be further increased, both in persistent luminescent powders, ceramics and single crystals.

Table of Contents image

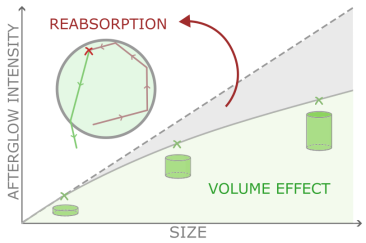

Persistent phosphors are luminescent materials that can emit light long after the excitation has ceased.[1,2] This technologically interesting feature follows from a photo-induced charge transfer between the activator dopant (e.g. Eu^{2+}) and a defect, often the trivalent lanthanide codopant like Dy^{3+} or Nd^{3+},[3,4] that acts as a metastable charge trapping center. Extensive research on these materials has started after the development of the green-emitting $SrAl_2O_4$:Eu,Dy a few decades ago.[5] Since then it has been proposed to use persistent phosphors for medical imaging,[6,7] theranostics,[8] remote thermometry,[9] structural health monitoring, photocatalysis and traffic or emergency signalization.[1]

A recent benchmarking study[10] including commercially available $SrAl_2O_4$:Eu,Dy powders and single crystals has shown that the integrated persistent luminescence intensity has not spectacularly increased since it was first reported in 1996. At the same time several independent experiments have shown that there is still a lot of room for improvement as only a few percent of the Eu centers are ionized at the same time in $SrAl_2O_4$:Eu,Dy [11,12] and

$Sr_4Al_{14}O_{25}$:Eu,Dy.[3] A straightforward way to overcome these fundamental limitations in performance is to move to transparent samples such as ceramics, glasses, polymer layers or single crystals.[13–15] In these materials a remarkable enhancement in persistent luminescence intensity can be achieved due to an increased phosphor volume. However, scattering should be minimized in order to optimize the light output making highly transparent single crystals, such as the ones used in this work, the preferred option.[16] Nevertheless, it is essential to suppress loss mechanisms which reduce the performance of the materials.

Recently, absorption of excitation light by trapped charges and the subsequent optically stimulated detrapping has been identified as a mechanism that dynamically limits the storage capacity of $SrAl_2O_4$:Eu,Dy [17,18] and $Sr_2MgSi_2O_7$:Eu,Dy[19] during photo-excitation of the phosphor. In the present work it is shown that some of these defects also introduce an absorption that strongly overlaps with the emission of the phosphor. As a result, part of the afterglow emission is absorbed by the trapped charges which are subsequently detrapped. This does not only negatively affect the integrated afterglow intensity but also considerably alters the kinetics of the afterglow decay.

This is substantiated by recording, analysing and modelling the afterglow emission of three cylindrical $SrAl_2O_4$:Eu,Dy single crystals with different sizes (diameter D = 5.0 mm, length L = 0.9, 2.4, 5.0 mm) but an identical composition (Figure 1d). To measure the afterglow (Figure 1a), the single crystals were mounted in an integrating sphere and exposed to high intensity blue light (445 nm, 125 mW/cm^2) for 15 minutes, which is sufficient to reach a steady state situation. As expected, the initial afterglow intensity of the crystals increases with size. However, this increase in intensity is not directly proportional to the size of the crystal and the larger crystals are dimmer than expected (full line in Figure 1). Additionally, with increasing size of the single crystals the afterglow decays faster and the integrated afterglow intensity per gram of the material, i.e. the so-called storage capacity,[11] decreases spectacularly by 42% (Figure 1b). The latter is also evident from the pictures in Figure 1d where the largest crystal, opposed to the two smaller crystals, is not visible anymore 165 minutes after excitation has ended.

As a consequence of the charge trapping process and the accompanying valence change of dopant ions, the optical absorption of the phosphor will change[17,20] and this will likely contribute to the size-dependence of the afterglow dynamics and intensity. These changes in absorption were identified by recording the transmission spectrum of the smallest single crystal before and after exposure to blue light (Figure 1c). To minimize undesired artefacts due to afterglow emission at room temperature, the transmission spectra were recorded at 75 K in a dedicated setup (Figure S1). However, excitation of the single crystal with blue light to induce charge trapping was performed at room temperature to overcome the thermal barrier for trapping.[21,22] A comparison of the transmission spectrum of the crystal in these two states, with empty traps or filled traps, reveals that an additional broad absorption band is created after excitation of the phosphor. No information could be obtained for wavelengths shorter than 485 nm as a long-pass filter was used to avoid excitation of Eu^{2+} during the measurement. However, the results imply that the trapped charges in the phosphor absorb light over a broad spectral range starting at an energy of 1.3 eV (950 nm) which is likely due to the $4f^{10} \rightarrow 4f^9 5d^1$ transition of Dy^{2+}[23–25] which will be the topic of a separate work. Moreover, this absorption strongly overlaps with characteristic green emission that can be ascribed to the $4f^6 5d^1 \rightarrow 4f^7$ transition of Eu^{2+} (Figure 1c).

While it is widely recognized that the absorption of light by trapped charges can result in optically stimulated detrapping, which is exploited in many applications including medical imaging or (personal) radiation dosimetry,[26–28] it should be noted that the mere absorption of light by these trapped charges does not guarantee subsequent detrapping. A notable example is CaF_2:Eu,Sm where a reversible electron transfer between the two dopants can be optically induced. The electron transfer from Eu to Sm creates several absorption bands in the vis-

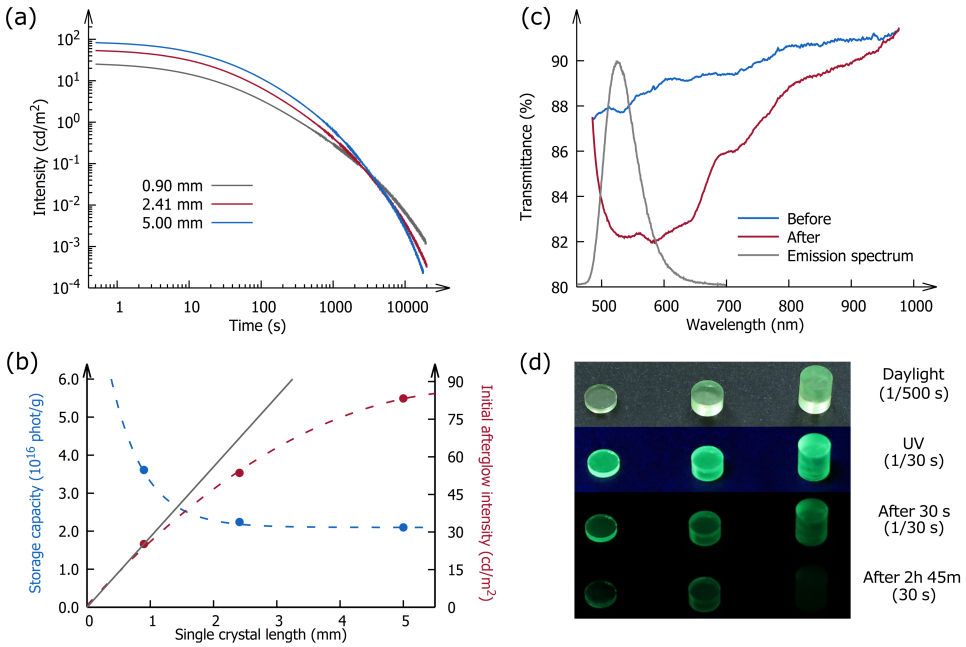

Figure 1: (a) Afterglow curves of the three $SrAl_2O_4$:Eu,Dy single crystals recorded after 15 minutes of excitation with blue (445 nm, 125 mW/cm^2) light. (b) The storage capacity and initial afterglow intensities of the three single crystals. The full grey line indicates the expected increase in initial intensity. The dashed lines are guides to the eye.(c) Transmission spectrum of the smallest crystal measured at 75 K along the axis of the cylinder, before and after exposure to blue light (445 nm, 6.5 mW/cm^2) for five minutes at room temperature. (d) Pictures of the three single crystals under different illumination and during afterglow recorded with a Canon EOS 6D Mark II (50 mm, f/4, ISO 800) with a variable integration time (indicated in the figure).

ible region coming from Sm^{2+}.[29] Yet, at room temperature, only excitation into the higher excited states of Sm^{2+} using violet (420 nm) light results in a significant transfer of the trapped electron back to Eu. Similar behaviour was also found in YPO_4:Ce,Sm but at lower temperature.[30]

So, to investigate whether (re)absorption of green light leads to optically stimulated detrapping in $SrAl_2O_4$:Eu,Dy the largest crystal was exposed to green laser pulses (532 nm, 300 mW/cm^2) while its afterglow was recorded (Figure 2c). It can be seen that exposure of the crystal to the green stimulation light results in a faster decrease of the afterglow intensity over time. The size of the effect depends on the length of the stimulation pulses.

Further convincing evidence can be found by looking at the effect of green light on the TL signal of the smallest single crystal. For this the crystal was illuminated with blue light (445 nm, 6.5 mW/cm^2) for five minutes. Ten minutes after the end of excitation the crystal was heated at a linear rate of 1 °C/s to record the TL signal. All shown TL profiles have been corrected for thermal quenching (TQ) (Figure 2d). The TL curve of the smallest single crystal (Figure 2a) is slightly asymmetric and peaks at 75 °C. If the crystal is exposed to green stimulation light (532 nm, 300 mW/cm^2) in the ten minutes between the end of excitation and the start of heating, the intensity of the TL curve decreases and the peak maximum slightly shifts to higher temperatures (77 °C). After 480 s of stimulation with green light, only 8% of the original intensity is left. The same experiment was repeated on commercially acquired $SrAl_2O_4$:Eu,Dy powder (Glotech, GT 8400) which was incorporated in a PDMS layer to ensure homogeneous exposure to the excitation and stimulation light. The TL curve of the powder sample peaks at 110 °C and is much broader than the glow peak of the single crystal. This is generally

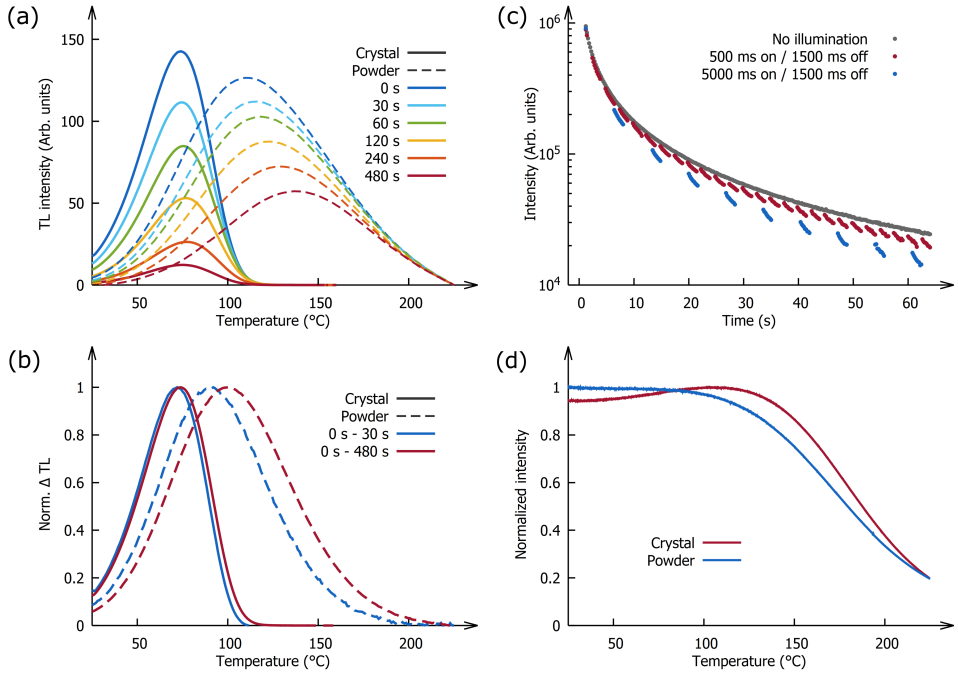

Figure 2: (a) Thermoluminescence curves of the smallest single crystal (L = 0.9 mm) and of powder, recorded at a heating rate of 1 °C/s and corrected for thermal quenching. Within the fixed ten minute time span between excitation (445 nm, 6.5 mW/cm^2, 300 s) and the start of recording the thermoluminescence glow curve, the samples were exposed to green light (532 nm, 300 mW/cm^2) for varying durations. (b) The difference between the TL curves recorded without exposure to green light and the ones recorded after 30 s (blue lines) or 480 s (red lines) of green illumination. (c) Afterglow of the largest single crystal (L = 5.0 mm) recorded after excitation with blue light (445 nm, 6.5 mW/cm^2) under pulsed stimulation with green light (532 nm, 300 mW/cm^2). The afterglow was only recorded when the green stimulation light was switched off. (d) Thermal quenching curves recorded under excitation with blue light (445 nm, 6.5 mW/cm^2) at a heating rate of 0.5 °C/s.

attributed to the wide trap depth distribution that can be present in persistent luminescent aluminates.[21,22,31,32] The difference between powders and single crystals is most likely due to a difference in synthesis conditions, sample composition and the use of boric acid. Upon exposure to green light the TL intensity of the powder likewise decreases, to about 43% of the initial intensity after 480 s of stimulation with green light. The low temperature side of the TL curve appears to be affected more and the contribution at higher temperatures is remarkably more stable under optical stimulation. As the green stimulation is prolonged, however, deeper traps are gradually depleted as well. This is visible in Figure 2b where the difference between the TL curves without and after 30 s or 480 s of illumination with green light is shown.

It can thus be concluded that part of the persistent luminescence from $SrAl_2O_4$:Eu,Dy single crystals and powders is absorbed by the trapped charges. Furthermore the reabsorption of the green emission induces further detrapping. The result is an accelerated depletion of the phosphor in combination with an apparently lower storage capacity because this optically stimulated detrapping process, that takes place in addition to the spontaneous thermally-driven detrapping, is essentially a loss mechanism, i.e. multiple traps are emptied per emitted photon. As such, the term storage capacity which is used to refer to the integrated afterglow intensity expressed in photons/gram should perhaps more suitably be called an *observable* storage capacity as it only relates to those trapped charges that result in detectable

light emission and is not equal to the concentration of trapped charges.

While the effect is smaller in powder samples compared to crystals, it might partially explain the difference between the storage capacities obtained by integrating the persistent luminescence of $SrAl_2O_4$:Eu,Dy powder[11] and the one obtained through X-ray absorption measurements[12] which was estimated to be roughly twice as large. A similar observation was made by Ueda *et al.*[14] who noted that the number of Yb^{2+} ions (i.e. presumably equal to the amount of trapped electrons) in a transparent $Y_3Al_2Ga_3O_{12}$:Ce,Yb ceramic, estimated through XANES and optical absorption measurements, was roughly a factor 55 higher than the number of photons emitted during afterglow. This was explained in the context of a reduced recombination efficiency with only a small fraction of the detrapped charges leading to emission upon recombination at the Ce activator. However, considering the transparency of the ceramic in combination to the strong Yb^{2+} absorption that is induced upon charging the phosphor and the overlap between this absorption and the Ce^{3+} emission it is likely that this discrepancy can also partly be attributed to losses due to reabsorption of the afterglow emission.

The absorption of emission light also has a considerable effect on the TQ profile recorded by heating the sample under constant illumination with blue light for the smallest single crystal (Figure 2d). The luminescence intensity initially increases, at temperatures where most of the trapped charges are already released, before the quenching finally sets in around 130 °C. The TQ profile is independent of the heating rate employed during the measurement (Figure S3) and it can thus be concluded that the increase in intensity is purely a consequence of a decrease in absorption because previously trapped charges are detrapped.

To elucidate the effect of the reabsorption of emission light on the dynamics and intensity of the afterglow of the three $SrAl_2O_4$:Eu,Dy single crystals, a three-dimensional ray-tracing model was implemented (Figure S2). A fixed number of emission centres were randomly distributed in the crystal. The concept of time is introduced in the model by including the trap depth ($E = 0.54$ eV) and frequency factor ($s = 1.15 \cdot 10^7$ s^{-1}) extracted from a variable heating experiment on the smallest crystal (Figure S4). This information is used to determine how many charges (n') spontaneously detrap every second according to the Arrhenius equation

$$n' = (N \cdot V) \cdot s \cdot e^{-\frac{E}{kT}} \tag{1}$$

where k is the Boltzmann constant, T is the temperature, N is the number density of trapped charges and V is the volume of the crystal.

The emission of every photon (E, Figure 3a) occurs in a random direction and the path of the photon in the crystal is calculated. If the angle of incidence at the surface is smaller than the critical angle, determined by the refractive index of $SrAl_2O_4$:Eu,Dy ($n = 1.6$),[33] the photon escapes the crystal. This is the case for all photons emitted within the blue cone in Figure 3a. If the angle is larger than the critical angle the photon is instead reflected (R). The distance traveled in the crystal before the photon is absorbed, is randomly generated from the distribution

$$\rho(\ell) = N\sigma \cdot e^{-\ell N\sigma} \tag{2}$$

where ℓ represents the path length and σ the extinction cross-section. If the photon escapes the crystal before reaching the selected absorption path length, no absorption occurs. However, if the path length is exceeded (i.e. the distance from E to A is larger than ℓ) than a photon is absorbed and an additional charge is detrapped (A). A new photon is emitted in a randomly generated direction again (red line and cone in Figure 3). Some degree of scattering at the crystal surface (S) is introduced into the simulation to avoid that photons are trapped infinitely in the crystal when the absorption becomes low. The probability for scattering is 1% at every reflection and if scattering takes place, the direction in which the photon travels after reflection is randomly changed by at most 1% in every direction. To simulate the impact of the slightly rounding of the edges encircling the cylinder bases (Figure S6), any

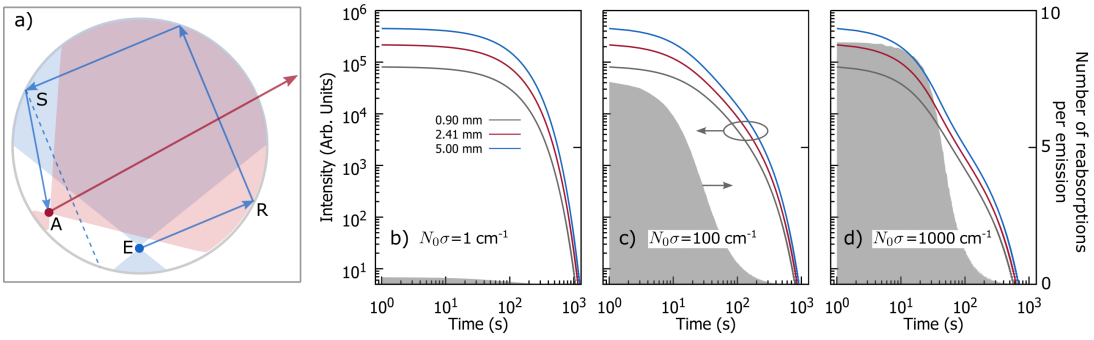

Figure 3: (a) Top view of a cross-section of a rod-shaped single crystal illustrating the concept of the ray tracing simulation. Colors and symbols are explained in the text. Simulated afterglow curves of the three cylindrical single crystals using three sets of parameters corresponding to weak (b), intermediate (c) and strong (d) absorption of the afterglow emission. The grey shaded area indicates how many reabsorption and emission events took place before a photon manages to escape the largest crystal (right axis).

photon that strikes the surface within a proximity of 0.2 mm from the edge does not undergo reflection but escapes the crystal. The model presented here does not include scattering of light within the crystal volume by the twin structures introduced by the phase transition occuring near 670 °C when cooling down.[34]

Afterglow curves have been simulated for three crystals with different sizes (Figure 3) using three different sets of effective parameters with $N_0\sigma$= 1, 100 and 1000 cm^{-1} where N_0 represents the initial number density of trapped charges. This corresponds to a weak, intermediate and strong absorption of afterglow emission, respectively. The first thing that stands out is that the simulated afterglow curves decay more rapidly than the experimental ones (Figure 1a), independent of the parameters that were used. This suggests that the trap depth measured during the variable heating rate experiment is likely too shallow. This underestimation is a result of the reabsorption of persistent luminescence, which also significantly affects the resulting glow curves. The simulation further indicates that the reabsorption of afterglow emission has a big influence on the shape of the afterglow curves and induces a large deviation from the mono-exponential decay that would be found in a material characterized by a single trap depth. With increasing absorption the decay speeds up and the integrated light intensity decreases, with only 87, 18 and 11% of the photons escaping the large crystal before absorption. The grey shaded area in Figure 3b-d indicates how many reabsorption and emission events take place for every charge that is thermally detrapped in the largest crystal. It is clear that this parameter varies over time which reflects the changes in absorption of the crystal as the number of trapped charges decreases. In the extreme cases, i.e. weak or strong absorption, the shape of the curves and the observable storage capacities are relatively independent on the size of the single crystals (Figure S5). In contrast, for an intermediate absorption of the afterglow emission, the smaller crystals decay notably slower than the larger ones and also the observable storage capacity becomes size-dependent with a significant decrease when comparing the largest to the smallest crystal.

Very similar observations can be made when looking at the experimental afterglow curves (Figure 1a). However, we are restricted to a qualitative comparison of the observed effects. It is impossible to draw quantitative conclusions from the simulation because this requires information about the actual defect concentrations. This information cannot straightforwardly be obtained via afterglow or TL measurements which are themselves heavily affected by the reabsorption. Neither is it possible to obtain the defect concentration from absorption measurements as this requires knowl-

edge about the chemical nature of the trapping defects, the associated oscillator strengths and the scattering characteristics of the crystals.

The fast luminescence decay observed during the first 100 seconds is consistent among all three single crystals. This size-independency of the decay rate can now be interpreted as a consequence of a strong reabsorption of the afterglow emission during this initial stage of the afterglow. As the material gradually depletes over time the number density of the trapped charges decreases, resulting in a lower absorption (Equation 2). After 100 seconds the decay curves start to exhibit a clear dependence on the size of the single crystal which resembles the simulated behaviour in case of an intermediate absorption of the afterglow emission. Most likely the afterglow curves will again exhibit the same characteristics, independent of size, when the crystals are sufficiently depleted but this probably occurs when the intensity of the afterglow is too low to be recorded by our experimental equipment. Overall the results agree well with the simulated afterglow curves. If the dimensions of the simulated crystal are reduced and the amount of scattering upon reflection at the surface is increased, resembling the conditions found in typical powder phosphors, the significance of the effect diminishes considerably, indicating that this effect will mainly have to be taken into account during the development of persistent luminescent single crystals, glasses or ceramics.

In conclusion, part of the afterglow emission in $SrAl_2O_4$:Eu,Dy is absorbed by filled traps which leads to an accelerated depletion of the larger crystals and a reduced observable storage capacity. This process can be regarded as a second loss mechanism, next to the already identified optically stimulated detrapping by excitation light. Its discovery further stresses the importance of investigating the optical properties of the trapping defects in persistent phosphors. To further improve the overall performance of large, transparent persistent luminescent materials it will be necessary to either introduce new trapping defects with other optical properties or to reduce the average path length of the light in the material. In the case of single crystals a more efficient outcoupling can be achieved by facetting the crystal to reduce the probability of total internal reflection or by moving towards a rougher surface which similarly limits total internal reflection.[13] For other transparent samples such as glasses or films this can also be achieved through the addition of scattering centers such as TiO_2 spheres[35] or pores.[36]

The results presented here underline that it is important to be careful when interpreting the meaning of trapping parameters obtained from a set of TL measurements on large transparent samples because the reabsorption of emission light introduces potential discrepancies between experimentally obtained trap depths and frequency factors and those those describing the actual underlying detrapping dynamics. Furthermore, the strong dependency of this effect on the exact morphology of the sample (surface polishing, size, shape) implies that it is not obvious to extrapolate results obtained on powder materials to large transparent samples. Finally, in the context of dosimetric and medical imaging applications, the reabsorption of afterglow, optically stimulated luminescence or TL presents an additional layer of complexity. The potential non-linearity induced by reabsorption can result in reduced sensitivity at higher doses, possibly preceding the onset of non-linear effects due to limited storage capacity. Understanding these implications is vital for optimizing the performance and accuracy of dosimetric applications, shedding light on the intricate interplay between reabsorption and the resulting response to varying doses. Moreover, the effect of reabsorption by trapped charges on the resulting emission intensity and efficiency also needs to be considered for applications where trapping defects are unwanted but might be present by accident, especially in the case of high-brightness applications.[37,38]

Nevertheless, exploiting the volume effect in (semi-)translucent samples still provides a promising avenue to enhance the overall emission intensity of afterglow materials.

Supporting Information

Additional experimental details and methods; block-diagram containing details of the simulation; thermal quenching curves recorded at various heating rates; results of a variable heating

rate experiment performed on the smallest single crystal to obtain the trapping parameters.

Conflict of interest

One of the authors (DR) is co-owner of BREVALOR, the company that developed the single crystals used in the present publication. The crystals were provided for research purposes, with no financial or other restrictions attached to their use.

Acknowledgements

The authors acknowledge the Research Foundation of Flanders (FWO) for financial support in the form of research project G0F9322N and the French Agence Nationale de la Recherche in the form of research project ANR-18-CE08-0012 PERSIST.

References

[1] D. Poelman, D. Van der Heggen, J. R. Du, E. Cosaert, and P. F. Smet; Persistent phosphors for the future: fit for the right application; *J. Appl. Phys.*; **2020** *128*; 240903.

[2] J. Xu and S. Tanabe; Persistent luminescence instead of phosphorescence: history, mechanism, and perspective; *J. Lumin.*;**2019**; *205*;581–620

[3] J. J. Joos, K. Korthout, L. Amidani, P. Glatzel, D. Poelman, and P. F. Smet; Identification of Dy^{3+}/Dy^{2+} as electron trap in persistent phosphors; *Phys. Rev. Lett.*; **2020**; *125*; 033001

[4] J. Kong and A. Meijerink; Identification and quantification of charge transfer in $CaAl_2O_4$:Eu^{2+},Nd^{3+} persistent phosphor; *Adv. Opt. Mater.*; **2023**; *11*(15); 2203004

[5] T. Matsuzawa, Y. Aoki, N. Takeuchi, and Y. Murayama; A new long phosphorescent phosphor with high brightness, $SrAl_2O_4$:Eu^{2+},Dy^{3+}; *J. Electrochem. Soc.*; **1996**; *143*(8); 2670–2673

[6] T. Maldiney, A. Bessiere, J. Seguin, E. Teston, S. K. Sharma, B. Viana, A. J. J. Bos, P. Dorenbos, M. Bessodes, D. Gourier, D. Scherman, and C. Richard; The in vivo activation of persistent nanophosphors for optical imaging of vascularization, tumours and grafted cells; *Nat. Mater.*; **2014**; *13*(4);418–426

[7] V. Castaing, E. Arroyo, A. I. Becerro, M. Ocana, G. Lozano, and H. Miguez; Persistent luminescent nanoparticles: Challenges and opportunities for a shimmering future; *J. Appl. Phys.*; **2021**; *130*(8); 080902

[8] H. Terraschke, M. Franzreb, and C. Wickleder; Magnetism and afterglow united: synthesis of novel double core-shell Eu^{2+}-doped bifunctional nanoparticles; *Chemistry - A European Journal*, **2020**; *26*(30); 6833-6838

[9] Z. Wu, L. Li, X. Lv, H. Suo, C. Cai, P. Lv, M. Ma, X. Shi, Y. Yang, L. Marciniak, and J. Qiu; Persistent luminescence ratiometric thermometry; *Chem. Eng. J.*; **2022**; *438*; 135573

[10] D. Van der Heggen, J. J. Joos, A. Feng, V. Fritz, T. Delgado, N. Gartmann, B. Walfort, D. Rytz, H. Hagemann, D. Poelman, B. Viana, and P. F. Smet; Persistent luminescence in strontium aluminate: A roadmap to a brighter future; *Adv. Fun. Mater.*; **2022**; *32*(52); 2208809

[11] D. Van der Heggen, J. J. Joos, D. Rodríguez Burbano, J. Capobianco, and P. F. Smet; Counting the photons: determining the absolute storage capacity of persistent phosphors; *Materials*; **2017**; *10*(8); 867

[12] K. Korthout, K. Van den Eeckhout, J. Botterman, S. Nikitenko, D. Poelman, and P. F. Smet; Luminescence and x-ray absorption measurements of persistent $SrAl_2O_4$:Eu,Dy powders: Evidence for valence state changes; *Phys. Rev. B*; **2011**; *84*(8); 085140

[13] T. Delgado, D. Rytz, G. Cai, M. Allix, E. Veron, I. di Carlo, and B. Viana; Highly transparent Ce^{3+},Cr^{3+} co-doped GYAGG single crystals with enhanced persistent luminescence; *Ceram. Int.*; **2023**; doi: 10.1016/j.ceramint.2023.02.249

[14] J. Ueda, J. Xu, S. Takemura, T. Nakanishi, S. Miyano, H. Segawa, and S. Tanabe; How many electron traps are formed in persistent phosphors?; *ECS J. Solid State Sci. Technol.*; **2021**; *10*(11),116003

[15] V. Castaing, C. Monteiro, A. D. Sontakke, K. Asami, J. Xu, A. J. Fernández-Carrión, M. G. Brik, S. Tanabe, M. Allix, and B. Viana; Hexagonal $Sr_{1-x/2}Al_{2-x}Si_xO_4$:$Eu^{2+}$,$Dy^{3+}$ transparent ceramics with tuneable persistent luminescence properties; *Dalton Trans.*; **2020**; *49*(46); 16849–16859

[16] Y. C. Lu, L. Chen, Q. Y. Zhang, B. A. Goodman, W. Deng, D. K. Xiong, and S. L. Xu; Luminescence and microstructural characteristics of Eu_2O_3-doped $SrAl_2O_4$ single crystals; *J. Lumin.*; **2023**; *253*; 119472

[17] D. Van der Heggen, J. J. Joos, and P. F. Smet; Importance of evaluating the intensity dependency of the quantum efficiency: impact on LEDs and persistent phosphors; *ACS Phot.*; **2018**; *5*(11); 4529–4537

[18] W. Jia, H. Yuan, S. Holmstrom, H. Liu, and W. M. Yen; Photo-stimulated luminescence in $SrAl_2O_4$:Eu^{2+},Dy^{3+} single crystal fibers; *J. Lumin.*; **1999**; *83-84*; 465–469

[19] C. Tydtgat, K. W. Meert, D. Poelman, and P. F. Smet; Optically stimulated detrapping during charging of persistent phosphors; *Opt. Mater. Express*; **2016**; *6*(3); 844

[20] D. Van der Heggen, R. Zilenaite, E. Ezerskyte, V. Fritz, K. Korthout, D. Vandenberghe, J. De Grave, J. Garrevoet, L. Vincze, D. Poelman, J. J. Joos, and P. F. Smet; A standalone, battery-free light dosimeter for ultraviolet to infrared light; *Adv. Fun. Mater.*; **2021**; *32*(14); 2109635

[21] H. Hagemann, D. Lovy, S. Yoon, S. Pokrant, N. Gartmann, B. Walfort, and J. Bierwagen; Wavelength dependent loading of traps in the persistent phosphor $SrAl_2O_4$:Eu^{2+}, Dy^{3+}; *J. Lumin*; **2016**; *170*; 299–304

[22] J. Botterman, J. J. Joos, and P. F. Smet; Trapping and detrapping in $SrAl_2O_4$:Eu,Dy persistent phosphors: Influence of excitation wavelength and temperature; *Phys. Rev. B*; **2014**; *90*(8); 085147

[23] N. Spector, J. Sugar, and J. F. Wyart; Analysis of the third spectrum of dysprosium (Dy III); *J. Opt. Soc. Am. B*; **1997**; *14*(3); 511–521

[24] M. Karbowiak, C. Rudowicz, and J. Cichos; The high-Resolution 4f-5d absorption spectrum of divalent dysprosium (Dy^{2+}) in strontium chloride host $SrCl_2$: fine structure and zero-phonon transitions revealed; *J. Phys. Chem. A*; **2018**; *122*(4); 923–928

[25] P. Dorenbos; A review on how lanthanide impurity levels change with chemistry and structure of inorganic compounds; *ECS J. Solid State Sci. Technol.*; **2013**; *2*(2); R3001–R3011

[26] E. G. Yukihara, S. W. S. McKeever, C. E. Andersen, A. J. J. Bos, I. K. Bailiff, E. M. Yoshimura, G. O. Sawakuchi, L. Bossin, and J. B. Christensen; Luminescence dosimetry; *Nat. Rev. Methods Primers*; **2022**; *2*(1); 26

[27] S. W. S. McKeever, M. S. Akselrod, L. E. Colyott, N. A. Larsen, J. C. Polf, and V. Whitley; Characterisation of Al_2O_3 for use in thermally and optically stimulated luminescence dosimetry; *Radiat. Prot. Dosim.*; **1999**; *84*(1-4); 163–168

[28] P. Leblans, D. Vandenbroucke, and P. Willems; Storage phosphors for medical imaging; *Materials*; **2011**; *4*(6); 1034–1086

[29] J. J. Joos, D. Van der Heggen, L. Amidani, L. Seijo, and Z. Barandiaran; Elucidation of the electron transfer mechanism in Eu^{2+} and Sm^{3+} codoped CaF_2: A step towards better understanding of trapping and detrapping in luminescent materials; *Phys. Rev. B*; **2021**; *104*(20); L201108

[30] A. J. J. Bos, N. R. J. Poolton, J. Wallinga, A. Bessiere, and P. Dorenbos; Energy levels in YPO_4:Ce^{3+},Sm^{3+} studied by thermally and optically stimulated luminescence; *Rad. Meas.*; **2010**; *45*(3-6); 343–346

[31] T. Aitasalo, J. Hölsä, H. Jungner, J. C. Krupa, M. Lastusaari, J. Legendziewicz, and J. Niittykoski; Effect of temperature on the luminescence processes of $SrAl_2O_4$:Eu^{2+}; *Rad. Meas.*; **2004**; *38*(4-6); 727–730

[32] P. Zeng, X. Wei, M. Yin, and Y. Chen; Investigation of the long afterglow mechanism in $SrAl_2O_4$:Eu^{2+}/Dy^{3+} by optically stimulated luminescence and thermoluminescence; *J. Lumin.*; **2018**; *199*(11); 400–406

[33] Y. Imai, R. Momoda, and C. N. Xu; Elasticoluminescence of europium-doped strontium aluminate spherical particles dispersed in polymeric matrices; *Mater. Lett.*; **2007**; *61*; 4124–4127

[34] S. Ito, S. Banno, K. Suzuki, and M. Inagaki; Phase transition in $SrAl_2O_4$; *Z. Phys. Chem.*;**1977**; *105*(3-4); 173–178

[35] V. Castaing, M. Romero, J. Torres, G. Lozano, and H. Miguez; Scattering spheres boost afterglow: a Mie glass approach to go beyond the limits set by persistent phosphor composition; *Adv. Opt. Mater.*; **2023**; 2301565; doi: 10.1002/adom.202301565.

[36] P. Zheng, S. Li, T.-L. Zhou, Y.-R. Xu, R.-J. Xie; Unique design strategy for laser-driven color converters enabling superhigh-luminance and high-directionality white light; *Laser Photonics Rev.*; **2019**; *13*; 1900147

[37] P. Zheng, S. Li, T. Takeda, J. Xu, K. Takahashi, R. Tian, R. Wei, L. Wang, T. Zhou, N. Hirosaki, and R.-J. Xie; Unraveling the luminescence quenching of phosphors under high-power-density excitation; *Acta Mater.*; **2021**; *209*; 116813

[38] P. Pichon, F. Balembois, F. Druon, P. Georges; 3D luminescent concentrators; *Opt. Express*; **2019**; *29*; 6915-6926